PHYSICAL REVIEW B VOLUME 29, NUMBER 11 1 JUNE 1984

Positron study of the Fermi surface of a $Nb_{50}Mo_{50}$ disordered alloy

C. R. Bull, J. H. Kaiser, A. Alam, N. Shiotani,* and R. N. West
School of Mathematics and Physics, University of East Anglia, Norwich NR4 7TJ, United Kingdom
(Received 30 January 1984)

The Fermi surface of a $Nb_{50}Mo_{50}$ disordered alloy has been studied by two-dimensional angular correlation of positron-annihilation radiation. The measured Fermi surface is well defined and several dimensions of the ellipsoidal hole pocket at N have been determined. The results are compared with the predictions of various alloy band calculations.

During the last few years our understanding of the electronic structure of disordered alloys has been deepened by important advances in theory and in experiment. In electron-energy band calculations[1] both the coherent potential (CPA) and average t-matrix (ATA) approximations can quantify the effects of disorder in terms of the resultant blurring of the E vs $\vec{k}$ dispersion curves and thus the Fermi surface. Both suggest there can sometimes be a relatively well-defined Fermi surface in the most concentrated of alloys. In experiment, the measurement of the two-dimensional electron-positron momentum space density[2] for an appropriately orientated single crystal and its transformation into an equivalent Bloch wave $\vec{k}$-space density via the Lock-Crisp-West (LCW) method[3] allows these effects to be directly and easily studied.

In the one-electron approximation, the transformed density can be defined[4] as

$$F(k_x,k_y)=\int dk_z \sum_{\text{occ. } \vec{k},n} \chi(n,\vec{k}) \ . \tag{1}$$

Here, n is an electron energy-band index, $\vec{k}$ the reduced Bloch wave vector, and the integral in k_z taken over a complete symmetry element in $\vec{k}$ space. The $\chi(n,\vec{k})$ are matrix elements involving the underlying electron and positron wave functions. In the approximation that the positron wave function is a constant[4] $\chi(n,\vec{k})$ are also constant and independent of n and $\vec{k}$ and $F(k_x,k_y)$ is simply the once-integrated electron $\vec{k}$-space density whose discontinuities define the Fermi surface. In reality, the positron wave function cannot be constant, but even then, as theory suggests[5] and experiments confirm, the $\chi(n,\vec{k})$ are usually sufficiently weak and smoothly varying functions of $\vec{k}$ within each band, and sufficiently similar in magnitude throughout the conduction bands, for $F(k_x,k_y)$ to approximate closely to the conduction electron $\vec{k}$-space density. Finally, and most importantly, it is known that neither the single-particle nor the many-particle[6] effects of the positron can shift the breaks in $F(k_x,k_y)$ that mark the Fermi surface.

This paper reports the first measurement of $F(k_x,k_y)$ in a concentrated transition-metal alloy $Nb_{50}Mo_{50}$ of sufficient precision to enable a quantitative assessment of some Fermi-surface parameters. The Nb-Mo system forms a continuous range of disordered solid solutions. This solubility is in accord with the results of augmented-plane-wave (APW) calculations[7,8] which predict very similar electronic band structures for Nb and Mo, particularly in the energy range between the two Fermi energies. The clear implication that Nb_xMo_{100-x} alloys form a close to rigid-band system has received further support from explicit alloy calculations by Nakao and Wakoh ($x=20,50,80$ in ATA),[9] by Colavita *et al.* ($x=20,50,80$ in CPA),[10] and by Donato *et al.* ($x=25,50,75$ in CPA).[11] All three calculations are in close agreement in respect to the essential topology of the $Nb_{50}Mo_{50}$ Fermi surface and differ only as to the detailed geometry and definition of the various Fermi-surface sheets. They all predict an ellipsoidal hole surface centered on N, an octahedral hole surface at H, a closed electron surface of nearly octahedral shape at Γ, and a closed electron surface near the midpoint of the ΓH axis.

Several positron studies of the Nb-Mo system have already been reported. Two-dimensional angular correlation measurements in our laboratory[12] on Nb, $Nb_{90}Mo_{10}$, $Nb_{70}Mo_{30}$, and Mo and a study of $Nb_{75}Mo_{25}$ by Manuel *et al.*,[13] have established the general trends in the change of the Fermi-surface topology across the system. More recent one-dimensional studies of $Nb_{80}Mo_{20}$ and $Nb_{50}Mo_{50}$ have been made by Shiotani, Okada, Sekizawa, and Nakamichi.[14] Their results were generally consistent with a rigid-band picture but, because of the inherent limitations of the one-dimensional (1D) measurement no quantitative discussion of Fermi surface parameters was possible.

The single crystal of $Nb_{50}Mo_{50}$ for this study was grown by zone melting in an argon arc furnace and was cut and mounted so that the resolved momentum components would lie in the (110) plane. The measurement was made at a specimen temperature of 40 ± 2 K in the University of East Anglia (UEA) 2D machine which is described in detail elsewhere.[15] An accumulation $\sim2.6\times10^9$ coincidence counts ($\sim2.3\times10^5$ counts at peak) gave a raw spectrum with the expected reflection symmetries about the [001] and [$1\bar{1}0$] directions. Accordingly, following correction for the instrumental momentum sampling function,[15] the spectrum was folded about these high-symmetry directions during construction of $F(p_x,p_y)$ by the usual superposition procedure.[3] The result is shown in the upper half of Fig. 1 together with the outline of the first Brillouin zone.

To aid our analyses of these data we have performed a complementary calculation of the same p_z integral of the conduction electron $\vec{k}$-space density. The band-structure calculation used the Korringa-Kohn-Rostoker (KKR) method and the virtual crystal approximation (VCA). The Nb and Mo potentials were constructed with the Mattheiss prescription[16] from Herman and Skillman[17] charge densities and assumed electron configurations of $4d^45s^1$(Nb) and $4d^55s^1$(Mo). The Slater exchange parameter α was set equal to 1. The calculated two-dimensional (2D) electron

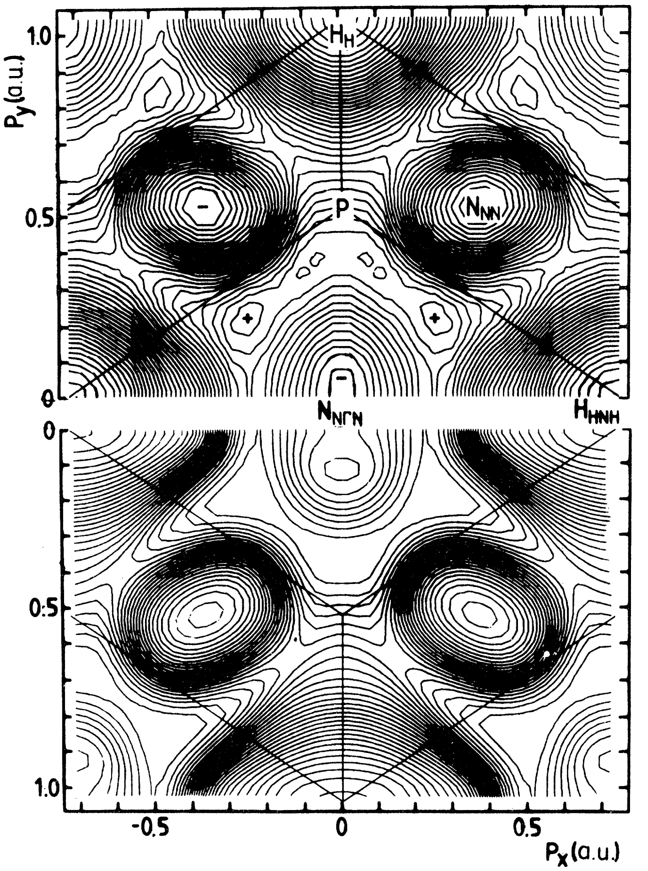

FIG. 1. Experimental once-integrated (integration direction [110]) two-dimensional electron-positron $\vec{k}$-space density (upper half) and the corresponding theoretical electron $\vec{k}$-space density (lower half) for a $Nb_{50}Mo_{50}$ alloy. The solid lines show the outlines of the first Brillouin zone and the subscripts on the N and H points define the integration path through the zone along the [110] direction. The theoretical density has been convoluted with a two-dimensional Gaussian of FWHM 0.09 a.u. to simulate the effects of the experimental resolution. The contour intervals are evenly spaced at 0.04 of the maximum amplitude variation. The local maxima and minima are marked appropriately.

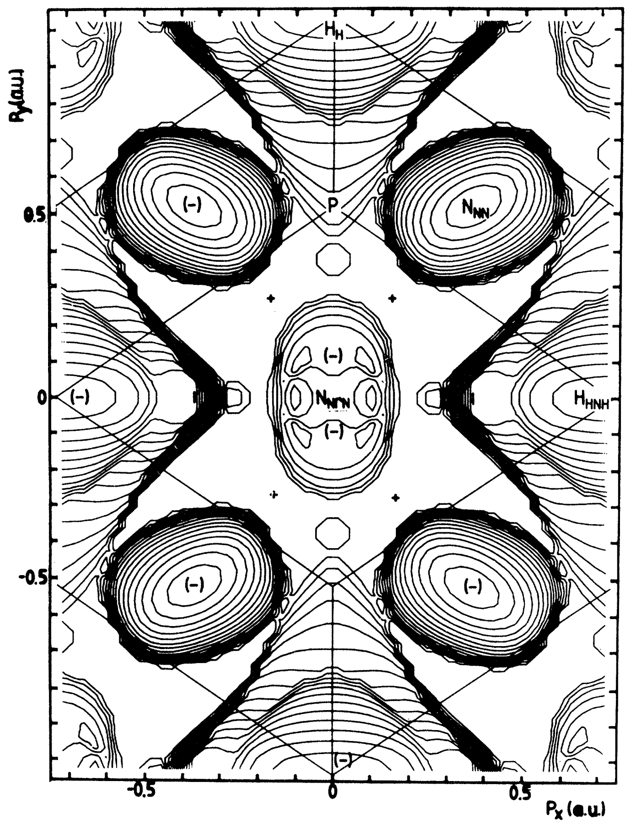

FIG. 2. Theoretical (once-integrated) electron $\vec{k}$-space density for $Nb_{50}Mo_{50}$. Apart from the contour intervals which have been arbitrarily chosen the presentation is the same as in Fig. 1. The fringing effect in some of the contours is not physical but merely an artifact of the plotting procedure.

$\vec{k}$-space density, which amounts to $F(k_x,k_y)$ with $\chi(n,\vec{k})=1$ for $4d$ and $5s$ electrons and zero otherwise [Eq. (1)] is shown in Fig. 2.

The result of the convolution of this function with a 2D Gaussian of full width at half maximum (FWHM) 0.09 a.u., which represents our best estimate of the overall experimental resolution, forms the lower half of Fig. 1.

The overall similarity between the two halves of this figure is remarkable. In each the same essential topology and major Fermi-surface sections are readily apparent. It should be recognized at this point that because these maps result from integration along the [110] direction various different parts of the original three-dimensional (3D) density are superimposed. The consequent degeneracy which is more apparent in Fig. 2 is indicated by the subscript notation. The only Fermi-surface sections not obscured by this effect are the ellipsoidal pockets at N_{NN}. For that reason we shall confine our quantitative analysis to them in this short report.

An overall resolution of 0.09 (± 0.01) a.u. is our best estimate of the combined effects of positron temperature,[2] instrumental resolution, and the data processing on our final results. Within this there is good correspondence between the theory and the experiment in respect to the definition of the hole pocket at N, a correspondence which is rapidly lost if the simulated resolution is significantly (e.g., 0.11 a.u.) worsened. Thus the indication is, at this preliminary stage,

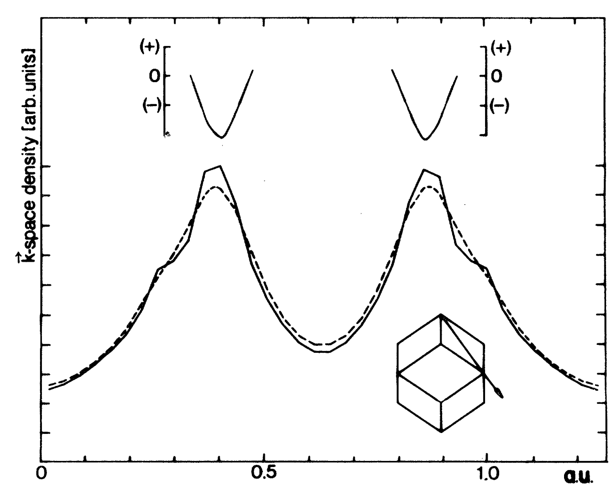

FIG. 3. Cross section through the N_{NN} point of the unconvoluted (solid line) and resolution convoluted (broken line) theoretical electron $\vec{k}$-space density. The plane of the cross section is indicated in the lower inset. The second derivative of the convoluted curve is also shown.

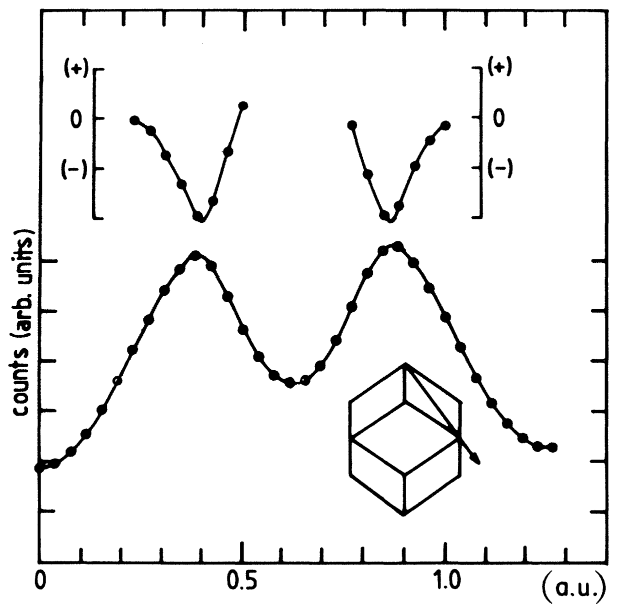

FIG. 4. Cross section through the experimental electron-positron $\vec{k}$-space density. The cross section in question and the presentation is as for Fig. 3.

that if there is any intrinsic disorder-induced blurring of the Fermi surface in this region, it is certainly less than 0.1 a.u. and probably somewhat smaller. In this the results are consistent with those of the earlier cited[9–11] theoretical calculations. The mean Fermi momenta can also be compared.

Analysis of our VCA theoretical curves reveals (Fig. 3) that the second derivative of the convoluted curve has its extrema at the singular Fermi-surface points of the unconvoluted version. In the light of this result the second derivatives of several cross sections of the experimental results through the N_{NN} points were calculated and the positions of their minima (Fig. 4) taken as the mean Fermi-surface parameters. The results together with the estimated uncertainties and the corresponding VCA parameters are presented in Table I. The agreement between the experiment and the simple VCA theory is now quantified and is clearly excellent. A further direct comparison between the experimental parameters and the predictions of the more sophisticated alloy calculations is ruled out by the lack of Fermi-surface caliper data along the appropriate directions (see table) in the published reports. However, the close correspondence between our experiment and our theory suggests the value of an indirect comparison of the Fermi-surface parameters along the $\overline{N\Gamma}$, $\overline{NH}$, and $\overline{NP}$ axes. These parameters, readily available from the present VCA results, can also be estimated from some of the Fermi-surface and dispersion curve figures of the earlier literature. Since both the ATA and CPA give blurred Fermi-surface *mean* values for the parameters were read from those figures. Within the precision of this procedure the results of Shiotani *et al.* (rigid band),[14] of Nakao and Wakoh (ATA),[9] and the present VCA theory were indistinguishable. The CPA calculations of Donato *et al.*[11] predict much larger caliper values, quite inconsistent with our data. The figures in Ref. 11 were inadequate for our purpose.

TABLE I. Apparent diameters of the ellipsoidal hole at N_{NN} through various cross sections of the two-dimensional $\vec{k}$-space densities. The different cross sections are indicated by the same subscript notation as used in Fig. 1.

	Expt. (a.u.)	VCA (a.u.)
P-N_{NN}-P	0.518 ± 0.016	0.526
$N_{N\Gamma N}$-N_{NN}-$N_{N\Gamma N}$	0.521 ± 0.019	0.526
H_{HH}-N_{NN}-H_{HNH}	0.463 ± 0.010	0.457
N_{NN}-N_{NN}-N_{NN}	0.437 ± 0.026	0.431

We should like to acknowledge considerable financial support from The Science and Engineering Research Council in this work. Thanks are also due to the Yamada Science Foundation for providing a travel grant to one of us (N.S.), to Professor T. Nakamichi, who kindly supplied the Nb-Mo specimen, and to S. G. Usmar, who contributed some technical assistance.

*On leave from the Institute of Physical and Chemical Research, Wakoshi, Saitama 351, Japan.

[1]S. Faulkner, Prog. Mater. Sci. 27, 1 (1982).

[2]S. Berko, in *Electrons in Disordered Metals and at Metallic Surfaces*, NATO Advanced Study Institutes Series, Series B, Physics, Vol. 42, edited by P. Pharisean, B. L. Gyorrfy, and L. Scheire (Plenum, New York, 1979), pp. 239–91.

[3]D. G. Lock, V. H. C. Crisp, and R. N. West, J. Phys. F 3, 561 (1973).

[4]D. G. Lock and R. N. West, Appl. Phys. 6, 249 (1975).

[5]J. H. Kaiser *et al.* (unpublished).

[6]C. K. Majumdar, Phys. Rev. 140, A227 (1965).

[7]S. Wakoh, Y. Kubo, and J. Yamashita, J. Phys. Soc. Jpn. 38, 416 (1977).

[8]N. Shiotani, T. Okada, H. Sekizawa, S. Wakoh, and Y. Kubo, J. Phys. Soc. Jpn. 43, 1229 (1977).

[9]Y. Nakao and S. Wakoh, J. Phys. Soc. Jpn. 51, 2840 (1982); 52, 3122 (1983).

[10]E. Colavita, A. Franciosi, R. Rosei, F. Sacchetti, E. S. Giuliano, R. Ruggeri, and D. W. Lynch, Phys. Rev. B 20, 4864 (1979).

[11]E. Donato, B. Ginatempo, E. S. Giuliano, R. Ruggeri, and A. Stancanelli, Phys. Status Solidi B 110, 39 (1982).

[12]R. N. West, in *Physics of Transition Metals*, Institute of Physics Conference Series No. 55 edited by P. Rhodes (IOP, Bristol, 1980), p. 35.

[13]A. A. Manuel, L. Oberli, T. Jarlborg, R. Sachot, P. Descouts, M. Peter, in *Positron annihilation*, edited by P. G. Coleman, S. C. Sharma, and L. M. Diana (North-Holland, Amsterdam, 1982), p. 281.

[14]N. Shiotani, T. Okada, H. Sekizawa, and T. Nakamichi, J. Phys. Soc. Jpn. 52, 2858 (1983).

[15]R. N. West, J. Mayers, and P. A. Walters, J. Phys. E 14, 478 (1981).

[16]L. F. Mattheiss, Phys. Rev. 133, A1399 (1964).

[17]F. Herman and S. Skillman, *Atomic Structure Calculations* (Prentice Hall, New York, 1963).